Comparisons of different methods to determine correlation applied to multi-port UWB eleven antenna

Comparisons of Different Methods to Determine Correlation Applied to Multi-Port UWB Eleven Antenna

Xiaoming Chen*, Per-Simon Kildal*, Jan Carlsson+

*Signals and Systems Department, Chalmers University of Technology
Gothenburg, Sweden
xiaoming.chen@chalmers.se

+Electronics department SP Technical Research Institute of Sweden
Boras, Sweden

***Abstract*— In this paper, we compare different methods to determine correlation. First, we did analytical study on correlation of two parallel dipoles. We present two methods for analytical correlation calculation. In addition, the effect of source impedances is also studied. It is found that these two analytical methods result in the same correlation, and that source impedance matched to embedded element impedance gives the smallest correlation. Then, we compared different methods of determining correlations of multi-port antennas from measurements. Wideband eleven antenna was used for measurements. It is shown that correlation can be determined correctly either using embedded radiation far field functions based on anechoic chamber (AC) measurement (i.e., embedded far field method), or using cross-correlation definition based on reverberation chamber (RC) measurement (i.e., RC method). Scattering parameters (S-parameter) can only be used to determine correlation of lossless multi-port antenna (i.e., S-parameter method). It is also shown that for general lossy antenna, RC method is most convenient to use.**

I. INTRODUCTION

Multi-port antennas have drawn considerable interest for improving wireless communications as diversity or MIMO terminal antennas. For mobile communications compact multi-port antennas are usually desired, which makes correlations between different antenna ports inevitable. Since correlations have adverse effects on diversity gain [1] and multiple-input multiple-output (MIMO) capacity [2], it is of interest to know the correlations. In the literature, there are different correlation definitions. In summary, the most common correlations are power correlation (cross-correlation of the received signal powers of two elements), envelope correlation (cross-correlation of the received signal amplitudes of two elements) and complex correlation (cross-correlation of the received complex signals of two elements). It is first shown in [3] that power correlation is equal to the magnitude square of complex correlation, and approximately equal to envelope correlation. In this paper, we will only use complex correlation. In early literature, mutual coupling in the multi-port antenna was neglected. The resulting correlation could then be called spatial correlation [2]. In [4] it is shown that under certain conditions (that we later will explain actually rarely appear in practice) the correlation of actual multi-port antenna can be obtained using equivalent impedance circuit model based on a priori knowledge of spatial correlation (Z-parameter method). A more direct method is to use embedded far fields of the multi-port antenna to calculate correlation by radiation field function multiplication and integration (embedded-far-field method) [5]-[6]. Embedded far-field functions are easily measured for all practical multi-port antennas. In this paper, we will compare these two methods using parallel dipoles as an example. In addition, we will show that source impedance conjugate matched to embedded element impedance gives negligible correlation as already concluded in [7]-[9].

Besides analytical study of correlation, we also present and compare different methods for measuring it in practice. The correlation can be calculated correctly using embedded far field method based on anechoic chamber (AC) measurement or using cross-correlation based on channel measurements in reverberation chamber (RC) measurement (RC method). Scattering parameters (S-parameter) can also easily be used for correlation calculation (S-parameter method [10]-[12]). However, the S-parameter method is valid only for lossless multi-port antennas [12]. In this paper, wideband eleven antenna [13] is used for measurements in AC and RC. It will be shown that for lossy multi-port antennas, RC method is most convenient in practice.

It is important to note that the overall performance of a MIMO system is given in terms of the maximum available capacity, and that both the embedded radiation efficiency and correlation contribute to reducing this. The capacity results for the same antenna and AC and RC measurement methods can be found in [14], whereas the present paper studies in more detail the correlation, including in addition results obtained by Z-parameter method.

II. CORRELATION OF PARALLEL DIPOLES

The equivalent circuit of the parallel dipoles is shown in Fig. 1. In this paper, we assume three-dimensional (3-D) isotropic rich scattering environment. We also assume the half-wavelength dipoles are identical and located respectively at $y_1=-d/2$ and $y_2=d/2$ along y-axis, and that their source

impedances are the same.

A. Z-Parameter Method

In the absence of mutual coupling, spatial correlation is

$$\rho_{oc} = \int_0^{2\pi}\int_0^{\pi} |\vec{G}(\theta,\phi)|^2 \exp(jkd\sin\theta\sin\phi)\, p(\theta,\phi)\, d\theta d\phi \quad (1)$$

where $\vec{G}(\theta,\phi)$ is the complex far field function [15] of an isolated dipole at the origin in free space, k is wave number, d is the separation distance between the dipoles, and $p(\theta,\phi)$ is the probability density function (PDF) of the angular distribution. In 3-D isotropic environments,

$$p(\theta,\phi) = \frac{\sin\theta}{4\pi} \quad (0 \le \theta < \pi, \quad 0 \le \phi < 2\pi) \quad (2)$$

The fading correlation with mutual coupling presented can be analyzed via impedance matrix of the parallel dipoles, as presented in [16]. The signals (voltages) received by the two dipoles are

$$\mathbf{V} = diag(\mathbf{Z}_S)[\mathbf{Z} + diag(\mathbf{Z}_S)]^{-1}\mathbf{V}_{oc} \quad (3)$$

where $\mathbf{V}_{oc} = [V_1^{oc} \quad V_2^{oc}]^T$ and $\mathbf{V} = [V_1 \quad V_2]^T$ are open-circuit voltage and terminal voltage vectors respectively, $\mathbf{Z}_S = [Z_s \quad Z_s]^T$ is source impedance vector, and $\mathbf{Z}$ is the equivalent impedance matrix for the parallel dipoles, and *diag* denotes diagonal transformation, and the superscript T represents transpose. The entries of $\mathbf{Z}$ (free space self-impedance Z_{11} and mutual impedance Z_{12}) are given in [17]. Equation (3) can be rewritten as

$$\begin{bmatrix} V_1 \\ V_2 \end{bmatrix} = \begin{bmatrix} \alpha & \beta \\ \beta & \alpha \end{bmatrix} \begin{bmatrix} \vec{G}(\theta,\phi) \\ \vec{G}(\theta,\phi)\exp(jkd\cos\phi) \end{bmatrix} \quad (4)$$

where α and β are the corresponding entries of matrix $diag(\mathbf{Z}_S)[\mathbf{Z} + diag(\mathbf{Z}_S)]^{-1}$. The correlation with mutual coupling present is

$$\rho_{mc} = E[V_1 V_2^*] / \sqrt{E[|V_1|^2]E[|V_2|^2]} \quad (5)$$

where the superscript * represents complex conjugate. The terms in (5) can be expressed as

$$\begin{aligned} E[V_1 V_2^*] &= (|\alpha|^2 + |\beta|^2)\rho_r + 2\,\mathrm{Re}\{\alpha\beta^*\} + j(|\alpha|^2 - |\beta|^2)\rho_i \\ E[|V_1|^2] &= |\alpha|^2 + |\beta|^2 + 2\rho_r\,\mathrm{Re}\{\alpha\beta^*\} + 2\rho_i\,\mathrm{Im}\{\alpha\beta^*\} \\ E[|V_2|^2] &= |\alpha|^2 + |\beta|^2 + 2\rho_r\,\mathrm{Re}\{\alpha\beta^*\} - 2\rho_i\,\mathrm{Im}\{\alpha\beta^*\} \end{aligned} \quad (6)$$

where ρ_r and ρ_i are respectively the real and imaginary parts of spatial correlation ρ_{oc}.

B. Embedded Far Field Method

The isolated antenna patterns of the half-wavelength dipoles are [6]

$$\vec{G}_i(\theta,\phi) = -\hat{\theta}\frac{2C_k\eta\cos(\pi/2\cos\theta)}{k\sin\theta}\exp(jk\frac{d_i}{2}\sin\theta\sin\phi) \quad (7)$$

where i=1, 2, d_1=-d, d_2=d, $C_k = -jk/4\pi$, and η is free space wave impedance. The embedded radiation patterns are [6]

$$\begin{aligned} \vec{G}_{emb,1}(\theta,\phi) &= \vec{G}_1(\theta,\phi)I_1 + \vec{G}_2(\theta,\phi)I_2 \\ \vec{G}_{emb,2}(\theta,\phi) &= \vec{G}_1(\theta,\phi)I_2 + \vec{G}_2(\theta,\phi)I_1 \end{aligned} \quad (8)$$

From the equivalent circuit, when the excitation current at port 1 is unity, I_1=1, I_2=-Z_{12}/(Z_{11}+Z_s). The correlation at the ports of the dipoles is

$$\rho_{mc} = \frac{\iint_{4\pi} G_{emb,1}(G_{emb,2})^* d\Omega}{\sqrt{\iint_{4\pi}|G_{emb,1}|^2\, d\Omega \iint_{4\pi}|G_{emb,2}|^2\, d\Omega}} \quad (9)$$

where $G_{emb,i}$ is the $\hat{\theta}$ component of $\vec{G}_{emb,i}(\theta,\phi)$.

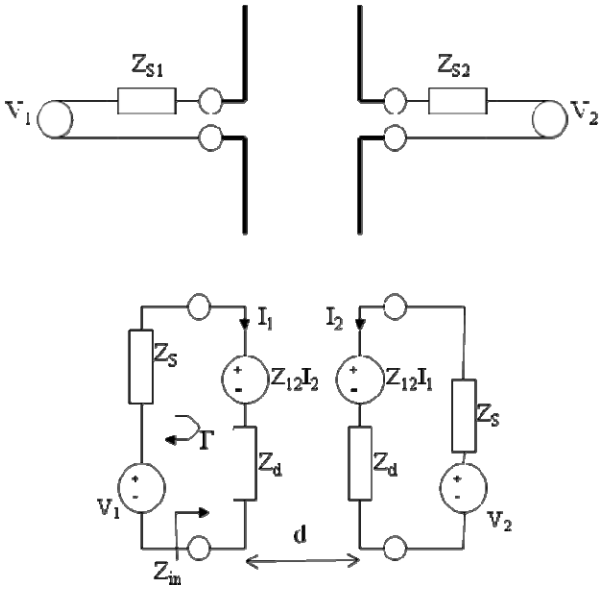

Fig. 1 Equivalent circuit for parallel dipoles.

C. Correlation Results

In this paper, we study three different source impedance cases: 50 Ω, conjugate matched to self-impedance, and conjugate matched to embedded element impedance. For half-wavelength dipoles, the self-impedance in free space is approximately 73+j42.5 Ω. From the equivalent circuit, embedded element impedance can be derived as

$$Z_{emb} = Z_{11} - \frac{Z_{12}^2}{Z_{11} + Z_s} \quad (10)$$

Substitute $Z_s = Z_{emb}^*$ into (10), we obtain two equations for the real and imaginary unknowns [8], [9]. The imaginary and real parts of the source impedance conjugate matched to embedded element impedance are [8], [9]

$$\begin{aligned} \mathrm{Im}\{Z_s\} &= \frac{\mathrm{Im}\{Z_{12}^2 - Z_{11}^2\}}{2\,\mathrm{Re}\{Z_{11}\}} \\ \mathrm{Re}\{Z_s\} &= \sqrt{\mathrm{Re}\{Z_{11}^2 - Z_{12}^2\} - 2\,\mathrm{Im}\{Z_{11}\}\,\mathrm{Im}\{Z_s\} - \mathrm{Im}\{Z_s\}^2} \end{aligned} \quad (11)$$

The correlations using Z-parameter and embedded far field methods with different source impedances are calculated and plotted as shown in Fig. 2. From Fig. 2, it is shown that the two methods give the same correlation, and that the pure spatial correlation for almost all distances is higher than the correlation with mutual coupling present. The agreement between the two methods means, in theory, that one can treat the spatial correlation and mutual coupling separately, provided the spatial correlation is calculated for the isolated single elements with the other element removed. Unfortunately, such spatial correlation can never be measured on a practical two-port antenna.

The separation of spatial correlation and the effect of mutual coupling is convenient for study of 2-D uniform scattering with omni-directional antennas, because in this case spatial correlation (1) reduce to Bessel function of zeroth order $J_0(kd)$, and correlation can be computed using Z-parameter method without any numerical integration. However, for 3-D isotropic scattering or with directive antennas, the integral (1) in Z-matrix method is generally unavoidable. The embedded far-field method, in this case, is more convenient, because it requires less computational efforts compared with Z-parameter method, and the embedded far-field can always be obtained for any multi-port antenna (if the ports are available for measurements).

It can also be seen from Fig. 2 that the source impedance has significant effect on correlation. It is shown that source impedance conjugate matched to embedded element impedance gives the smallest correlation. This agrees with [7] and [8]. We see also that setting the source impedance equal to infinity gives the spatial correlation, but this is only valid when we can make the induced current on the non-excited element zero by open-circuiting its non-excited ports. Generally, this is only possible when there is no transmission line connected between then radiating element and the port, and at the same time the elements themselves must be of single-mode type so that each one of them does not cause any scattering when the port is open-circuited (minimum scattering element antennas).

The low correlation for embedded impedance-matched case means that conjugate matching to embedded element impedance results in orthogonal far-field functions. However, it is pointed out in [9] that this optimum matching is achieved at the expense of bandwidth reduction. It is worth mentioning that within very small antenna separation the thin-wire assumption (that assumes current does not vary in azimuth around the wire) is not valid any more [18]. Therefore, both methods break down in this region. Nevertheless, the tiny small separation region is of little practical interest, and therefore does not affect the main conclusion of the paper.

III. Correlation of Eleven Antenna

The correlation measurements were done using the wideband so-called eleven antenna described in [13] and shown in Fig. 3. In this paper, the four ports for one polarization of the eleven antenna, shown in Fig. 3, are combined to two ports for one polarization as shown in Fig. 4 by using two wideband 180° hybrids. The result is a two-port antenna with ports P1 and P2 at which correlation is calculated. Each of the ports corresponds therefore to one log-periodic dipole array (one petal), and the log-periodic dipole arrays of the two ports P1 and P2 are parallel. The 180° hybrids have losses between 1.4 dB at 2 GHZ and 3 dB at 8 GHz.

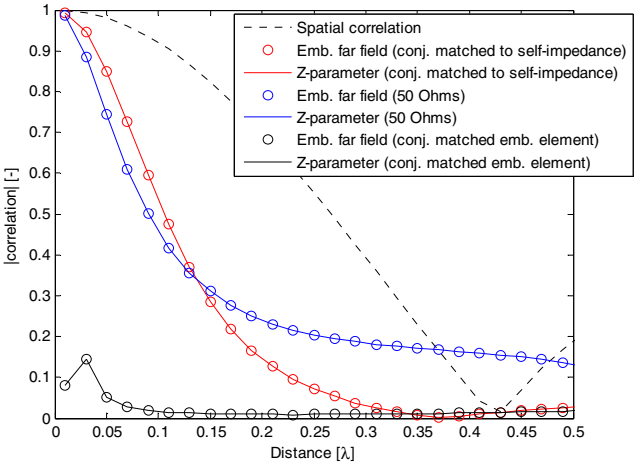

Fig. 2 Correlations using Z-parameter and embedded far field methods with different source impedances.

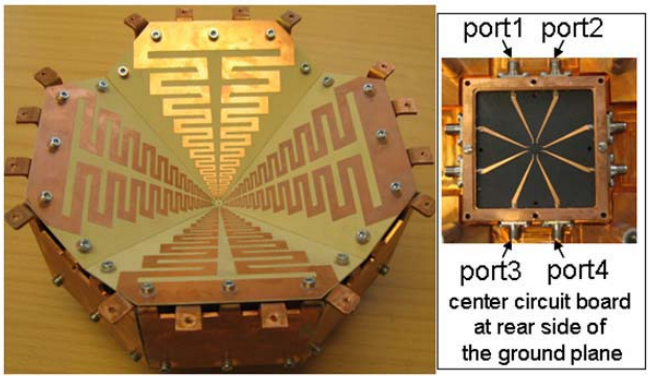

Fig. 3 Photos of front and back sides of Eleven antenna in use.

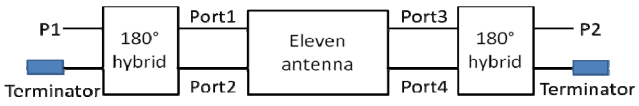

Fig. 4 Diagram of Eleven antenna combined as a two-element antenna.

A. *Embedded Far Field Method*

In practice, the embedded radiation far field can be measured in anechoic chamber (AC). The correlation using embedded far field method can be calculated using (9).

B. S-Parameter *Method*

Envelope correlations based on S-parameters for two-element and multi-element antennas has be derived separately by Blanch [10] and Thaysen [11]. The complex correlation can be easily derived using similar procedure based on [12]

$$\rho = \frac{-(S_{11}^* S_{12} + S_{21}^* S_{22})}{\sqrt{(1-|S_{11}|^2 - |S_{21}|^2)(1-|S_{22}|^2 - |S_{12}|^2)}} \quad (12)$$

In practice, the free-space S-parameters are also measured in AC. This method is called S-parameter method. The method seems very easy to use. However, it is valid only when the Ohmic losses in the antenna are negligible [12]. Note that the available S-parameters of the eleven antenna have been measured at the four ports, port1, port2, port3 and port4 (see Fig. 3) without hybrids. These measured S-parameters were combined using two ideal lossless 180° hybrids (similar like Fig. 3, except that the lossy hybrids are replaced by ideal lossless hybrids) to obtain S-parameters at "lossless" ports P1' and P2'. The S-parameters in (12) correspond to ports P1' and P2'. By doing this, we can exclude the hybrid losses.

C. RC *Method*

Apart from the two methods mentioned above, one can always calculate correlations based on the cross-correlation definition

$$\rho = \frac{E[V_1 V_2^*]}{\sqrt{E[|V_1|^2]E[|V_2|^2]}} \quad (13)$$

where V_i (i = 1, 2) is the complex signal received at ith element port in rich scattering environment. In order to (13), the number of independent samples should be large enough. A convenient way to gather so many independent samples is to measure eleven antenna in RC.

D. Measurements and Results

The RC in use is Bluetest HP reverberation chamber, with a size of 1.75 m × 1.25 m × 1.8 m. A sketch of it is shown in Fig. 5. In Bluetest RC, there are three wall antennas mounted at three orthogonal walls used for polarization stirring [19]. The antenna under test (AUT) is placed on a platform, which will rotate during measurements, referred to as platform stirring [19]. Two metal plates are used as mechanical plate stirrers, corresponding to the mode-stirrers in other RCs. In the measurements, the platform is moved to 20 positions spaced by 18°, and for each platform position each of the two plates move to 10 positions simultaneously, evenly along the total distance they can move. At each stirrer position and for each of the three wall antennas, a full frequency sweep is performed by the vector network analyzer (VNA). The RC emulates Rayleigh fading environment with 3-D isotropic angular distribution.

The embedded far fields of the eleven antenna are measured in AC at Technical University of Denmark. The S-parameters of the eleven antenna are measured in AC at Chalmers University of Technology. The complex signals of the eleven antenna are measured using Bluetest RC. In this paper, all the three methods mentioned above are used to calculate correlation of the eleven antenna.

Power correlation, envelope correlation and complex correlation can be calculated based on the definition of cross-correlation with the measured data in RC. Fig. 6 shows the different correlations measured in RC. It is shown that power correlation, magnitude squares of complex correlation and envelope correlation are basically equal to each other, which agrees with the analytical derivation in [3].

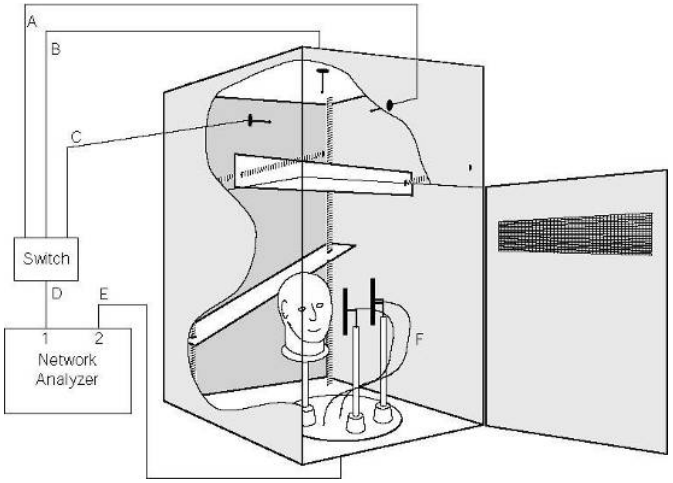

Fig. 5 Drawing of Bluetest RC with two mechanical plate stirrers, platform, three wall antennas and example of two-port antenna under test.

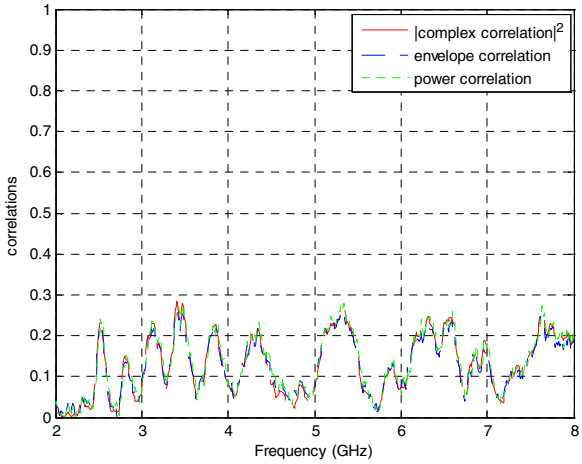

Fig. 6 Comparison of power correlation, envelope correlation and magnitude square of complex correlation based on RC measurements (different curves overlap).

The complex correlations are calculated by the three methods using (9), (12) and (13) based on corresponding measurements respectively and plotted in Fig. 7. It is shown from Fig. 7 that the measured correlations using embedded far field method and RC method agree with each other, but the correlation by S-parameter method deviates from the correlations by other methods. Nevertheless, it is worthy to point out that, while (12) is well known as a valid expression for correlation for lossless antenna, the disagreement is due to various practical reasons. For examples, the accuracy in measuring S_{11} has significant impact on correlation using (12); the real hybrid may affect the S-parameters more than simply power loss; finally when P1 and P2 are not excited coherently, the ohmic loss of antenna itself may not be negligible. The embedded far field method and RC method are valid for both lossless and lossy antennas; and they give the same result.

The frequency step for RC measurements is 1 MHz. A 20 MHz frequency stirring [21] is applied to improve RC measurement accuracy. Hence, the frequency resolution of the correlation by RC method is 20 MHz. The frequency resolution of the correlation by embedded far-field method is 100 MHz (the frequency step for embedded far-field measurements is 100 MHz). To use the embedded-pattern method for directive antenna, the angular resolution should be fine enough to give correct result. For embedded far field measurement in this paper, the angular resolution is 1°. By comparison, the RC method has a both better frequency resolution and required less measurement times. Therefore, RC method seems more convenient to use for measuring correlation of lossy multi-port antennas.

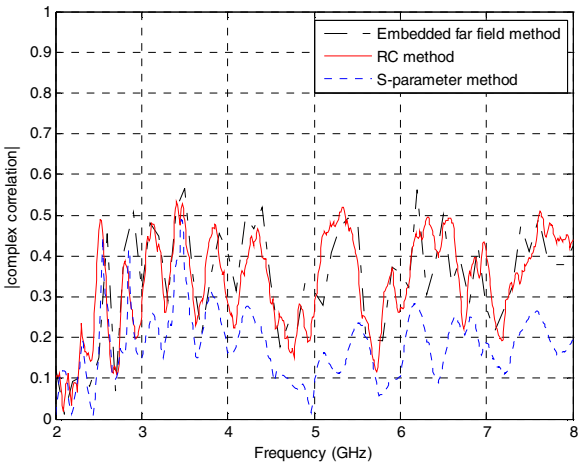

Fig. 7 Comparison of magnitudes of complex correlations using different methods.

IV. Conclusions

We have found that the Z-parameter method and embedded far field method gave the same correlation for analytical lossless parallel dipole antennas, and that conjugate matching the source impedance to the embedded element impedance gives almost zero correlation.

We have presented and compared three methods for determining correlations based on measurements of the multi-ort eleven antenna, when excited on two parallel dipole ports. The reverberation chamber (RC) method and embedded-far-field method work for both lossless and lossy antennas. Measurements in RC and anechoic chamber (AC) show that RC method and embedded far-field AC method agree very well with each other. In general, the RC method requires less measurement time, thus is more convenient to use for measuring correlation of lossy antennas.

Acknowledgment

This work has been supported in part by The Swedish Governmental Agency for Innovation Systems (VINNOVA) within the VINN Excellence Center Chase.

References

[1] K. Rosengren and P-S. Kildal, "Radiation Efficiency, Correlation, Diversity Gain and Capacity of a Six Monopole Antenna Array for a MIMO System: Theory, Simulation and Measurement in Reverberation Chamber," in *Proc. IEE, Microwaves, Optics and Antennas*, pp. 7-16, Vol.152, No.1, Feb 2005.

[2] D. Chizhik, F. Farrokhi, J. Ling and A. Lozano, "Effect of antenna separation on the capacity of BLAST in correlated channels," *IEEE Communication Letters*, vol. 4, no. 11, pp. 337-339, Nov. 2000.

[3] J. N. Pierce and S. Stein, "Multiple diversity with nonindependent fading", Proceddings of the IRE, pp. 89-104, 1960.

[4] R. Janaswamy, "Effect of element mutual coupling on the capacity of fixed length linear arrays," *IEEE Antennas and Wireless Propag. Lett.,* vol. 1, pp. 157-160, 2002.

[5] R. G. Vaughan and J. B. Andersen, "Antenna diversity in mobile communications", *IEEE Trans. Vehic. Technol.* vol. 36, no. 4, pp. 149-172, Nov. 1987.

[6] P.-S. Kildal and K. Rosengren, "Electromagnetic analysis of effective and apparent diversity gain of two parallel dipoles", *IEEE Antennas and Wireless Propag. Lett.,* vol. 2, pp. 9-13, 2003.

[7] J. W. Wallace and M. A. Jensen, "Termination-dependent diversity performance of coupled antennas: network theory analysis", *IEEE Trans. Antennas Propag.,* vol. 52, no. 1, pp. 98-105, Jan. 2004.

[8] K. Rosengren, J. Carlsson and P.-S. Kildal, "Maximizing the effective diversity gain of two parallel dipoles by optimizing the sources impedances", *Microwave and Optical Technology Letters,* Vol. 48, No 3, pp. 532-535, Mar. 2006.

[9] B. K. Lau, J. B. Andersen, G. Kristensson, and A. F. Molisch, "Impact of maching network on bandwidth of compact antenna arrays", *IEEE Trans. Antennas Propag.,* vol. 54, no. 11, pp. 3225-3238, Nov. 2006.

[10] S. Blanch, J. Romeu and I. Corbella, "Exact representation of antenna system diversity performance from input parameter description", *Electronics letters*, vol. 39, no. 9, pp. 705-707, May 2003.

[11] J. Thaysen and K. B. Jakobsen, "Envelope correlation in (N, N) MIMO antenna array from scattering parameters", *Microwave and optical technology letters*, vol. 48, no. 5, pp. 832-834, May 2006.

[12] S. Stein, "On cross coupling in multiple-beam antennas", *IRE Trans. Antennas Propagat*., pp. 548-557, Sep. 1962.

[13] J. Yang, M. Pantaleev, P.-S. Kildal, Y. Karadikar, L. Helldner, B. Klein, N. Wadefalk, C. Beaudoin, "Cryogenic 2-13 GHz eleven feed for reflector antennas in future wideband radio telescopes", to appear in *Special issue on Antennas for Next Generation Radio Telescopes in IEEE Transactions on Antennas and Propagation*, March 2011.

[14] X. Chen, P.-S. Kildal, J. Carlsson and J. Yang, "Comparison of ergodic capacities from wideband MIMO antenna measurements in reverberation chamber and anechoic chamber", resubmitted to *IEEE Antennas and Wireless Propagat. Lett.*, Feb. 2011.

[15] P.-S. Kildal, *Foundations of Antennas: A Unified Approach*, Studdentlitteratur, 2000.

[16] J. Luo, J. R. Zeidler and S. McLaughlin, "Performance analysis of compact antenna arrays with MRC in correlated Nakagami Fading channels*," IEEE Trans. Veh. Technol*., vol. 50, no. 1, pp. 267-277, Jan. 2001.

[17] C. A. Balanis, *Antenna theory: analysis and design*, 3rd edition John Wiley & Sons, 2005.

[18] A. C. Ludwig, "Wire-grid modeling of surfaces," *IEEE Trans. Antennas Propagat*., vol, 35, pp. 1045-1048, Sept. 1987.

[19] P.-S. Kildal and K. Rosengren, "Correlation and capacity of MIMO systems and mutual coupling, radiation efficiency and diversity gain of their antennas: Simulations and measurements in reverberation chamber", *IEEE Communications Magazine*, vol. 42, no. 12, pp. 102-112, Dec. 2004.

[20] J. Yang, S. Pivnenko, T. Laitinen, J. Carlsson, X. Chen, "Measurements of Diversity Gain and Radiation Efficiency of the Eleven Antenna by sing Different Measurement Techniques," *EuCAP 2010*, Barcelona, Spain, 2010.

[21] D. A. Hill, "Electronic mode stirring for reverberation chamber", *IEEE Trans. Electromagn. Compat.*, vol. 36, no.4, pp. 294-299, Nov. 1994.